Sādhanā (2020)45:260
https://doi.org/10.1007/s12046-020-01496-x

Heat and mass transfer analysis on multiport mini channel shelf heat exchanger for freeze-drying application

G SRINIVASAN and B RAJA*

Indian Institute of Information Technology, Design and Manufacturing, Kancheepuram, IIITDM Kancheepuram, Chennai 600 127, India
e-mail: srinivasang@iitg.ac.in; rajab@iiitdm.ac.in

MS received 25 January 2020; revised 24 June 2020; accepted 8 September 2020

Abstract. An experimental study on heat transfer characteristics of shelf heat exchangers, which are used in small-scale freeze dryers, is presented in this paper. The proposed heat exchanger consists of the multiport mini-channel flow paths, and a comparison with a conventional serpentine is carried out based on uniformity of the product temperature achieved. The experimental results indicate that the mini-channel shelf has better temperature uniformity than the latter. Skimmed milk is used as the test fluid. In the freezing and drying process, the product temperature variation is minimal in the mini-channel heat exchanger, with a variation of 12.5 % and 25%, respectively, and the heat transfer coefficient is found to be from 140 to 267 $Wm^{-2}\ K^{-1}$. The moisture content in the product reduces to 50 % in 2 hours, and the drying rate is higher at 0.032 kg hr^{-1} after 1 hour of the drying process. The redesign of the heat exchanger will be an essential tool to improve the performance with uniform temperature distribution on the product and to improve the product quality.

Keywords. Freeze drying; multiport mini channel; serpentine channel; shelf heat exchanger; heat transfer coefficient.

1. Introduction

Food and pharmaceutical industries extensively use freeze-drying for the manufacture of dry products with the residual moisture content less than 1%. The freeze-dried food product has the least thermal degradation and well retained the original flavor and aroma. A detailed review of the application of freeze-drying can be observed in the open literature [1–6]. Figure 1a, b and c show the schematics of the overall freeze-drying process in a P-T diagram, various stages, and isopropyl alcohol ramp-hold sequence. The process consists of three stages, namely freezing, primary drying, and secondary drying. In the freezing stage, the food product is kept on a tray and mounted on the top surface of the shelf heat exchanger. Heat exchange fluids like isopropyl alcohol, silicone oil, etc. are used as heat exchange fluids. It is necessary to freeze the product well below the eutectic or glass transition temperature [7]. It is needless to mention that the rate of freezing decides not only the size of ice crystals but also the mass transfer resistance and sublimation rate during the subsequent drying stage.

The freezing process can be divided into three regions, namely pre-cooling, phase change, and sub-cooling. Pre-cooling consists of super-cooling and nucleation. In super-cooling, the product remains in the liquid state well below the freezing point without phase change [8]. Nucleation initiates the phase change process, and it is followed by the sub-cooling phase. The extent of super-cooling depends on materials and cooling rate [9, 10]. Slow cooling rate results in the formation of larger ice crystals, which in turn makes the sublimation process quicker [11, 12].

The primary drying follows freezing, and during this stage, the temperature of the product is increased by a ramping and holding scheme. Around 85 to 95 % of the moisture content sublimates during primary drying [4, 5]. Upon further progressive heating, the remaining bounded water in the product is removed by desorption, and the product finally reaches the ambient temperature. A low-temperature condenser is used to condense the water vapor that is sublimated and desorbed.

In the overall freeze-drying process, the primary drying stage takes significant time. The driving forces for sublimation are the vapor pressure difference between the location of the evaporator (shelf heat exchanger) and condenser, mass transfer rate, and thermal diffusion [13, 14]. The major resistance for mass transfer occurs at the sublimating interface and from the dried region above the interface [15, 16].

The influence of thermal resistance in the heat flow path to the product affects the drying behaviour [17]. The conduction resistance and air gap resistance from the shelf to

*For correspondence
Published online: 15 October 2020

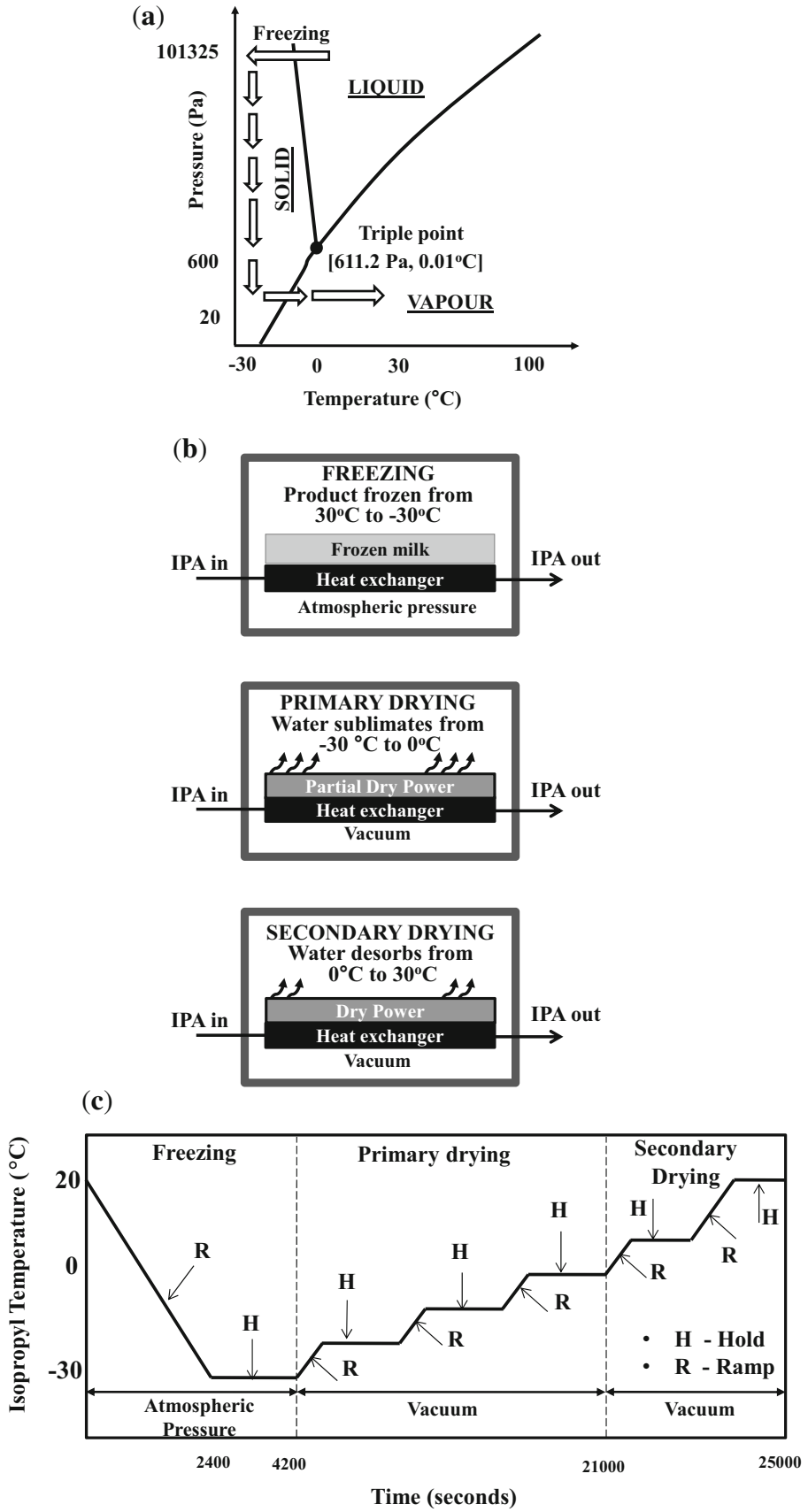
(a)
Freezing
101325
LIQUID
Pressure (Pa)
SOLID
Triple point
[611.2 Pa, 0.01°C]
600
20
VAPOUR
-30
0
30
100
Temperature (°C)
(b)
FREEZING
Product frozen from
30°C to -30°C
Frozen milk
IPA in
Heat exchanger
IPA out
Atmospheric pressure
PRIMARY DRYING
Water sublimates from
-30 °C to 0°C
Partial Dry Power
IPA in
Heat exchanger
IPA out
Vacuum
SECONDARY DRYING
Water desorbs from
0°C to 30°C
Dry Power
IPA in
Heat exchanger
IPA out
Vacuum
(c)
Isopropyl Temperature (°C)
Freezing
Primary drying
Secondary
Drying
20
0
-30
R
H
H
R
H
R
H
R
H
R
H
R
• H - Hold
• R - Ramp
Atmospheric
Pressure
Vacuum
Vacuum
2400
4200
21000
25000
Time (seconds)

◀**Figure 1.** (**a**) Pressure Temperature (PT) diagram of distilled water. (**b**) Different stages of Freeze drying process. (**c**) Ramping and holding sequence of isopropyl during dying process.

tray and radiation resistance affect the sublimation process [18]. Controlling heat input to product influences drying patterns and results in uniform temperature distribution throughout the product [19]. The heat input and chamber pressure are the control parameters to achieve better-dried products and to achieve inter-vial uniformity in vials placed on the shelf [20, 21].

1.1 *Serpentine and Multiport mini channel heat exchanger*

The conventional shelf heat exchangers used in the freeze-drying application are in a serpentine shape. The shelf heat exchangers of freeze-dryers consist of two stainless steel plates welded together. The bottom plate consists of the grooved fluid path (serpentine shape), and the upper plate is flat. The performance of the conventional freeze dryer is affected by the two major factors (air gap resistance and uniformity of product temperature). Firstly, the product to be dried is kept on a tray and mounted above the shelf heat exchanger. The heat exchange continuously maintains the product at the desired temperature. For practical reasons and easy access to the product, the tray is always slide-able or completely removable. Therefore, a vapor gap between the tray and the shelf heat exchanger is imminent, and the contact conductance may vary between 0.02 and 0.1 m^2 K/W [22]. The variation of contact thermal resistance (inverse of contact thermal conductance) between two metallic surfaces varies linearly and inversely concerning pressure [23]. Secondly, the quality of the freeze-dried product depends on uniformity in the temperature of the product on the tray above the shelf heat exchanger during the entire process. If the heat exchanger achieves non-uniform cooling, a similar non-uniform pattern will reflect in the product, which is kept on the tray above the heat exchanger. Hence as shown in Figure 1(c), it is required to ramp and hold the temperature of the isopropyl alcohol entering the heat exchanger until uniformity in temperature on the product is achieved along with homogeneity in the ice crystal structure and uniform heat and mass transfer. Thus, the use of vacuum pumps and low-temperature systems makes freeze-drying a costlier process. These are the essential design aspects concerning heat and mass transfer in a freeze dryer, which affects its performance.

To overcome the above factors, a mini channel shelf heat exchanger is proposed for freeze dryer application. Mini channels have played a vital role in electronic cooling devices for achieving a uniform heat transfer coefficient. The heat transfer rate during a transport process depends on the surface area to volume ratio. The surface area varies with the hydraulic diameter D for a channel, and the mass flow rate depends on the cross-sectional area, which varies linearly with D^2. Thus, the ratio of the surface area of the tube to its volume varies as 1/D, and as the diameter decreases, the ratio increases [24, 25]. The thermal resistance that prevails is also minimum. Thus, in the present work, shelf design using mini-channels is tested for the freeze-drying application to reduce the thermal resistance and achieve uniformity in product temperature. Fabrication of mini-channels in a freeze dryer shelf is a daunting task, but a possible option.

Even though enormous literature is available for freeze-drying concerning the product and the process, very few concerning the design aspects of the shelf heat exchanger in the freeze dryer machine for its effective heat transfer and power consumption is limited and is still very much open for new research. The objectives of the study are: (i) A comparison of product temperature in the serpentine and mini-channel shelf heat exchanger is carried out experimentally. (ii) The cooling curve behavior in a mini channel shelf heat exchanger is reported. (iii) The influence of chamber pressure and product temperature on drying behavior is analyzed. (iv)Determination of moisture content variation, drying time, and rate is carried out. (v) Determination of heat transfer coefficient and effectiveness of the heat exchanger is reported.

2. Test facility

Figure 3a shows the schematic layout of the test facility to study the heat transfer characteristics during freeze-drying. The main components in a freeze-drying apparatus are the product chamber (PC), condensing unit (CU), and temperature control bath (TCB). The three components are interconnected. The product chamber houses the shelf heat exchanger and tray. It consists of a temperature connector (TPC) and a vacuum gauge (VG) to measure the product temperature and pressure inside the product chamber. The Vacuum pump is connected to the condensing unit and product chamber.

The condensing unit (CU) consists of a blocking valve (BV), which is used to separate the product chamber and condensing unit from each other and assists in measuring the pressure drop (Δp). The vacuum bleed valve (VB) is opened at the end of the drying process to allow the atmospheric air inside. The condenser unit consists of a cooling coil to freeze the sublimated water vapor from the product into ice on its surface. The condensed vapor is drained at the end of the drying process using a water drain from the condensing unit. The condenser unit consists of a vacuum gauge to measure the pressure at the condenser unit.

The temperature-controlled bath is filled with heat exchange fluid isopropyl alcohol (IPA) and is pumped from a temperature-controlled bath, which is equipped with a

Table 1. Accuracies of the measured quantities.

Quantity	Description	Accuracy
Δm	Mass sublimated	± 0.3 grams
ΔT	Product Temperature	± 0.5 °C
Δi	Ice thickness	± 0.2 mm

microcontroller to maintain the temperature, and to the ramp and hold at the required time during various stages of the freeze-drying process. The temperature-controlled bath consists of a refrigerant unit (RU), which houses a condenser and evaporator. The isopropyl alcohol is cooled to the desired temperature in the refrigerant unit and heater unit and is passed through a magnetic pump (P) from the reservoir (R) to condenser unit through condenser line and to shelf heat exchanger present in product chamber through tray coolant line. During the freezing and drying process, the temperature of isopropyl alcohol is controlled at a ramping rate of 1.5 °C/min and 0.33 °C/min, respectively, in both configurations. However, during the freezing stage, ramping of heat exchange fluid (isopropyl alcohol) is carried out without holding. During drying stages, instead of continuously ramping the heat exchange fluid entering the heat exchanger, the fluid is maintained at a constant temperature (hold) for a fixed time to ensure uniformity in the product temperature and then ramped and kept in hold. This sequence is repeated, as shown in Figure 1c. The vacuum pressure and product temperature are measured continuously and are logged continuously using a data acquisition system.

The serpentine shelf and mini channel are designed, developed, and tested in the above-mentioned freeze-drying unit. The serpentine shelf heat exchanger consists of 8 passes, and each pass has one channel with a cross-section of 76 mm^2 (19*4), as shown in figure 2a. The proposed mini channel shelf heat exchanger used in the experimental set-up has 4 passes, and each pass has 8 mini channels with the size of (3*3) 9 mm^2 with a total cross-section of 8 mini channels at 72 mm^2 as shown in figure 2b. The hydraulic diameter of each channel is 3 mm. The length of both the channel is 280 mm.

3. Results and discussion

As discussed earlier, freeze-drying of skimmed milk is conducted in a laboratory-scale system using a multiport mini-channel shelf heat exchanger. The following sections consist of a comparison of transient variation of temperature in product between serpentine and mini-channel configuration. A detailed discussion on drying rate, time, heat load, heat transfer coefficient, and effectiveness of mini-channel configuration is done. The product everywhere in the text referred to as skimmed milk of 150 ml with 84 % (126 ml) water content. The uncertainty has been calculated, and the accuracies of the measured quantities are given in table 1.

3.1 *Comparison of product temperature uniformity in serpentine and mini-channel shelf heat exchanger*

The temperature of the product as a function of time is measured at similar locations (L1 L2 L3 and L4) in the serpentine and mini-channel shelf heat exchanger as shown in figure 3b. A comparison of temperature plot at various locations against the inlet isopropyl alcohol temperature (IPA) on the shelf is plotted for both the heat exchangers. The comparison of temperature plot in the freezing process (figures 4a and 4b) and drying process (figures 5a and 5b) are shown separately. The inlet of isopropyl alcohol during the freezing stage is lowered from 30 to −30 °C, and it represents a linear plot, as shown in Figures 4a and 4b. In an ideal case, the product temperature during the freezing stage must be similar to the inlet isopropyl alcohol temperature. In contrast, it can be observed that there exists a variation in product temperature in the serpentine and mini channel during the freezing process, and a similar trend is observed in drying stages. The bounds are created to show the variation range of product temperature with respect to the inlet temperature of isopropyl alcohol.

The temperature variation in the product during the freezing process is higher in the serpentine channel flow path with temperature variation up to 75 % and minimal in mini channel shelf with 25%, as shown in Figures 4a and 4b. In the case of the drying process, a similar observation is observed (figures 5a and 5b) with serpentine having a variation slightly higher than 25% when compared to mini channel shelf with less than 12.5%. During drying sequence, the IPA (Isopropyl Alcohol) in the bath is ramped from −30 °C to −20 °C in 30 min (0.33 °C/min) and it is held at −20 °C for next 20 min. This sequence of ramping 10 °C in 30 min and holding at that temperature of the next 20 min is repeated until the bath reaches 20 °C. This ramping and holding sequence is carried out to ensure that the product does not exceed the critical temperature and starts to melt. It can be inferred from the temperature plot (figures 5a and 5b) due to holding sequence in the drying process, the variation of temperature is minimal on both shelves when compared to the freezing process. Due to larger temperature variation in the freezing process in the serpentine channel, the corners of the product show a wavy structure and collapse at the end, whereas in the case of mini-channel, a smooth layer of ice pattern is seen throughout the shelf as shown in figures 6a and 6b. Hence during drying, the chances of a collapse are higher in the serpentine channel, whereas for the same test condition mini-channel shelf exchanger results in complete drying of the product. Hence the performance of a mini-channel shelf heat exchanger is discussed in detail in the present work.

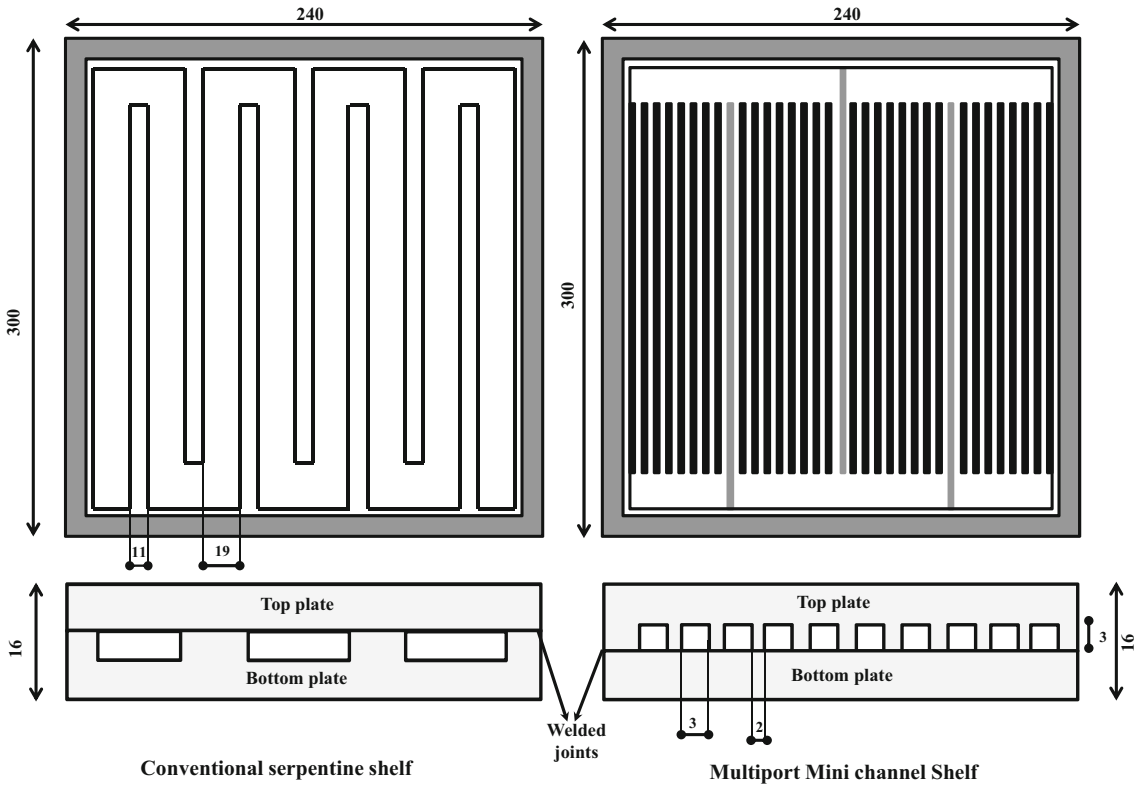

Figure 2. Conventional serpentine and proposed mini-channel shelf heat exchanger layout.

3.2 *Variation of product temperature and cooling curve behavior in a mini-channel shelf heat exchanger*

Figure 7 shows the averaged values of measured temperature at various locations on the product during the entire freeze-drying process using mini channel configuration. The three stages, which are freezing, primary and secondary drying, are demarcated in Figure 7. The freezing process is completed at 3420 s when the product reaches −30 °C and the drying regions are demarcated based on product temperature. Once the product temperature reaches 0 °C only desorption of water content starts. Hence it is made sure that all the frozen water molecules are sublimated before the product reaches 0 °C; hence no meltdown phenomena occur. During the entire drying process, no meltdown phenomena are observed. Primary drying is carried out till 21300 s, and secondary drying completed at 24129 s.

During the freezing stage, the skimmed milk at ambient temperature and pressure is progressively cooled and frozen to −30 °C. The cooling curve behavior of skimmed milk during progressive cooling is explained in the inset graph. It shows the temperature-time profile evolved during the cooling of the skimmed milk sample. Point '0' in the figure 7 indicates super-cooling of skimmed milk (−4 °C), where the product remains in the liquid phase, even below its freezing temperature without phase change. Crystallization starts after point '0' in the product. Point '1' in the inset graph shows the initial freezing point reached by the product due to the release of heat from crystallization. Subsequently, the skimmed milk loses its latent heat of fusion to solidify; hence the temperature remains constant during phase change. Upon completion of the phase change process, the temperature of the product drops further in the sub-cooling stage. To avoid meltdown phenomena in the drying process, the product is sub-frozen well below the critical point (point '2') as recommended. At this point, the inlet temperature to the shelf heat exchanger is maintained

Table 2. Measurement of water content sublimated and desorbed during drying process.

Sl. no	Time (s)	Sublimated and desorbed content in grams (skimmed milk—150 ml)
1	0	0
2	3600	33
3	7200	59
4	10800	80.1
5	14400	98
6	18000	112
7	21600	122
8	24129	126

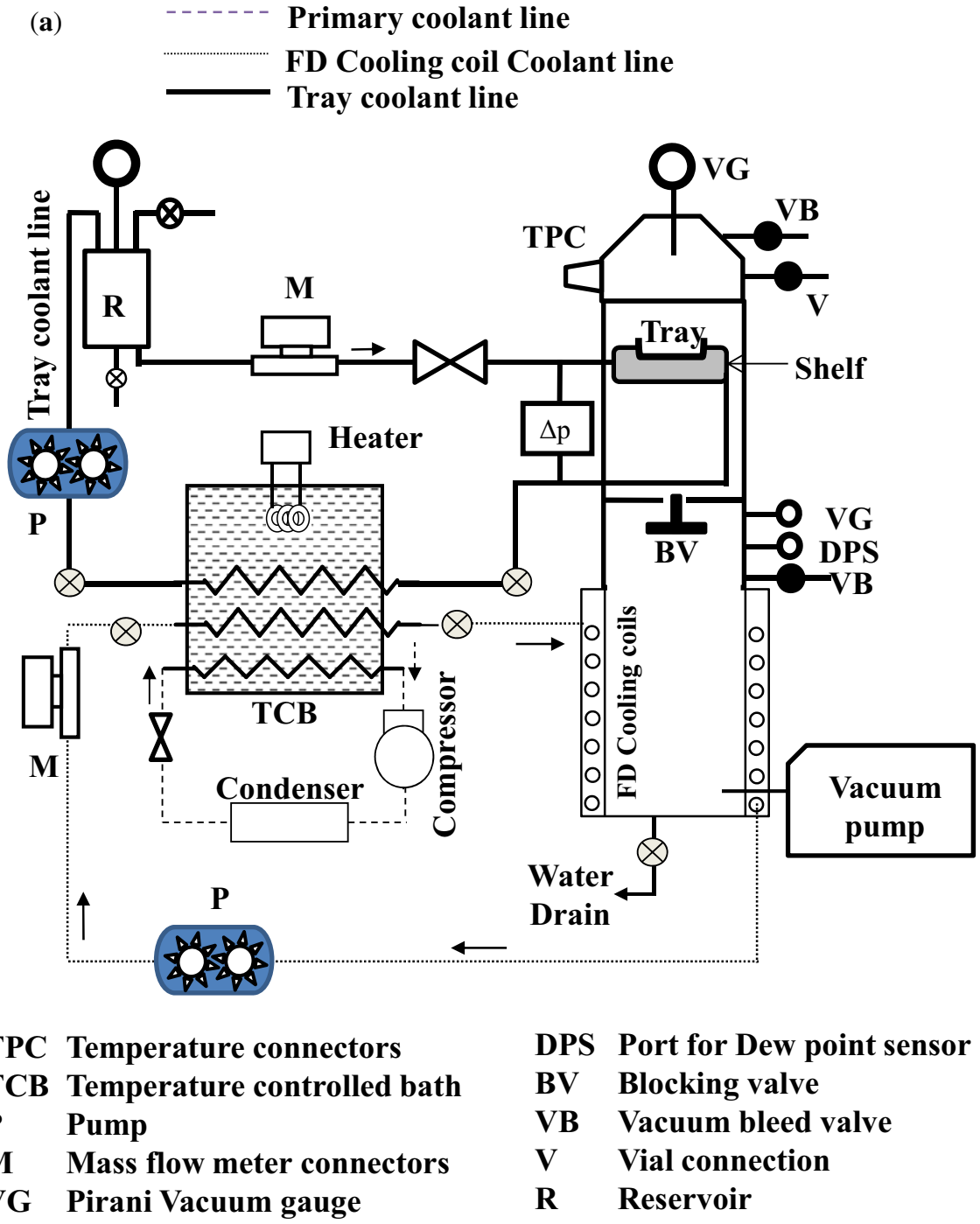

Figure 3. (**a**) Schematic layout of experimental set-up. (**b**) Location of temperature measured in the product (L1, L2, L3 and L4).

for a fixed time to ensure that the spatial variation of temperature with the product is negligible. At point '3', the sublimation process is ceased due to the absence of unbounded water molecules, and the product temperature exceeds the triple point. At point '4', the product temperature reaches a constant value, and the pressure in the chamber drastically reduces to the least value indicating the endpoint of the drying process.

3.3 *Influence of chamber pressure and product temperature on sublimation and desorption of water vapor*

Figure 8a shows the variation in chamber pressure against product temperature, and the variation in chamber pressure and product temperature against time is shown in figure 8b. In Figure 8a, the horizontal line (a-b) shows the

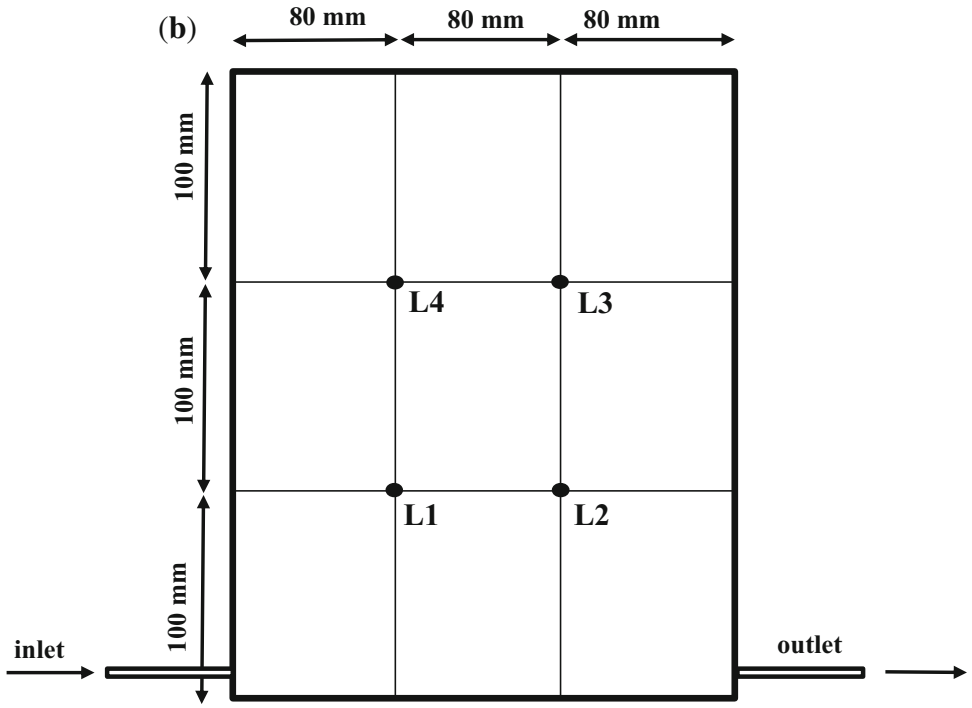

Figure 3. continued

temperature and pressure values during the freezing stage. The entire freezing process is carried out at atmospheric pressure, as shown in a horizontal line (a–b). The vertical line (b to 1) shows that atmospheric pressure is reduced to vacuum condition. Line 1 points the starting of the primary drying process (where sublimation of unbound water molecules start) or end of the freezing stage. Line 2 points the end of sublimation during the primary drying process (where unbound water (95%) content in the product is sublimated). Line 3 points the end of the secondary drying process (where bound water (5%) present in the product is desorbed). When the vacuum is introduced at the end of the freezing stage (point '1'), primary drying begins. The sublimation of frozen water takes place as the chamber pressure falls well below the triple point pressure of water (660 Pa and 0.01 °C). The chamber pressure at the beginning of drying is around 100 Pa, which is conducive for water molecules to sublimate from the top surface of the product. Since the vacuum pump continuously pulls the sublimated vapour towards the low-temperature condenser, the measured pressure in the chamber is the sum of the net effect caused by pressure rise due to sublimated vapour and the vacuum pressure created by the pump. In figure 8 b, the pressure rise against the time is steep at the initial stage, which is due to rapid sublimation at the surface directly exposed to vacuum. The pressure rise gradually decreases, which indicates the formation of a dried layer causing mass transfer resistance for sublimation to occur from the inner layer of the product. The latent heat of sublimation transports through the frozen layer and enables the sublimated water vapor to transport through the porous layer of dried material. By progressively ramping and holding the temperature of the product at various stages, the frozen water trapped in the subsequent inner layers of the product sublimates. The thickness of the drying layer progressively increases as the frozen layer reduces due to sublimation. Figures 8a and 8b show that the slope of the chamber pressure flattens and tend to decrease, which indicates that the sublimation dominant drying has ceased at point '2'. Again, the pressure of the chamber is well below the triple point pressure of water, but the product temperature has reached close to 0 °C due to progressive heating using the shelf heat exchanger. Once the temperature of the shelf heat exchanger exceeds the triple point temperature, the frozen water may melt and collapse the entire partially dried cake. Multiple trials of experiments are conducted to finalize the control scheme during the primary drying (Holding and Ramping) to avoid such a collapse.

It is important to sublimate the entire free water molecules, which is present in the form of ice, in the primary drying stage. Thus, a change in the slope of the chamber pressure against the time indicates the end of primary drying. In other words, the time at which there is no more frozen water and no scope for sublimation dehydration represents the end of the primary drying stage. Also, by referring to figures 8a and 8b, it can be observed that the primary drying takes most of the time out of the entire drying process. Upon continuation of ramping and holding

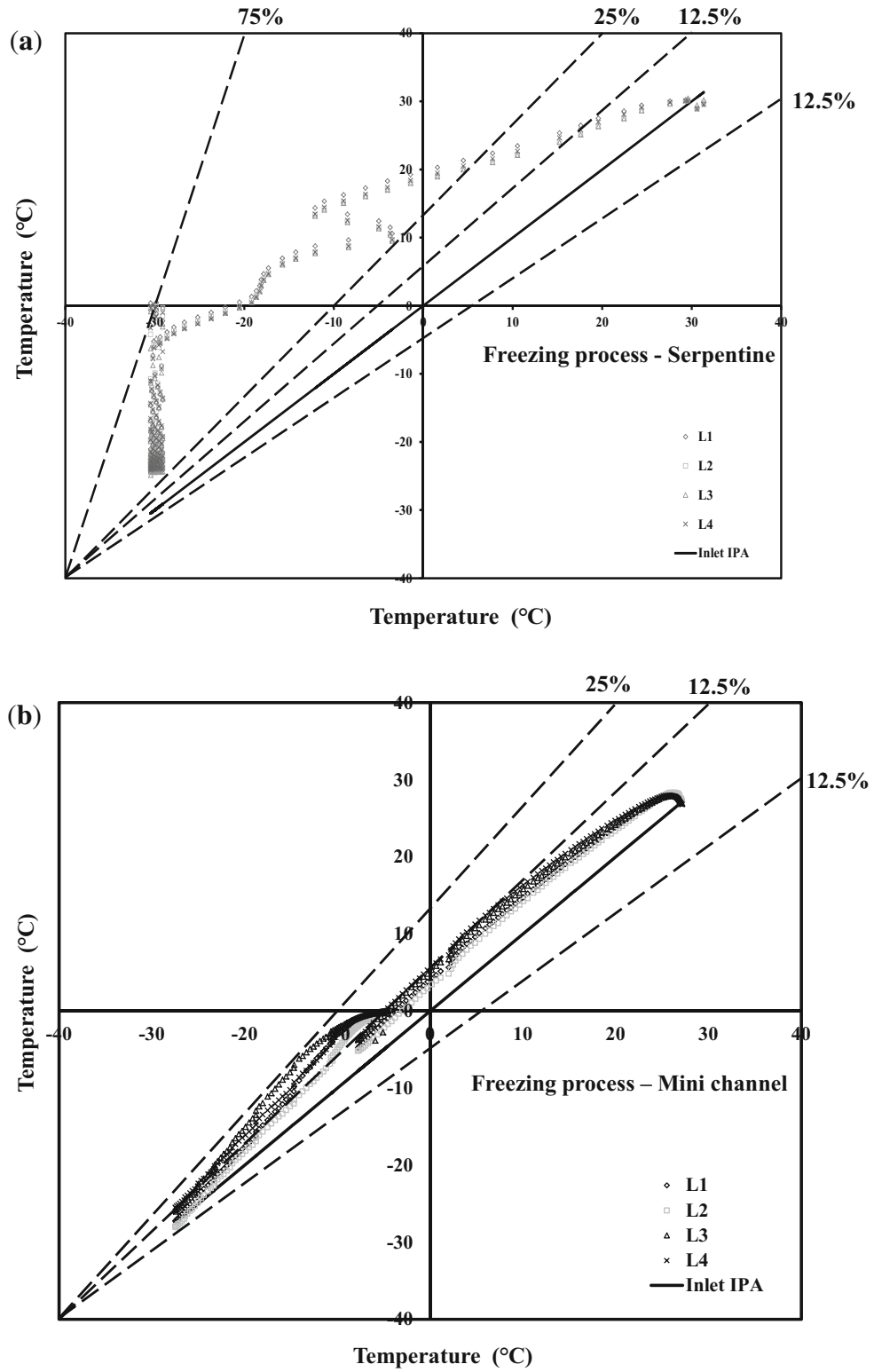

Figure 4. (**a**) Product temperature variation in freezing process—serpentine channel. (**b**) Product temperature variation in freezing process—mini-channel.

of the temperature of the shelf heat exchanger beyond the triple point temperature of the water, the desorption of remaining bound water takes place under vacuum. In figures 8a and 8b (point 3) show that a decrease in slope indicates that the quantum of water vapour released from the dried product is very less. Point 3 indicates that the

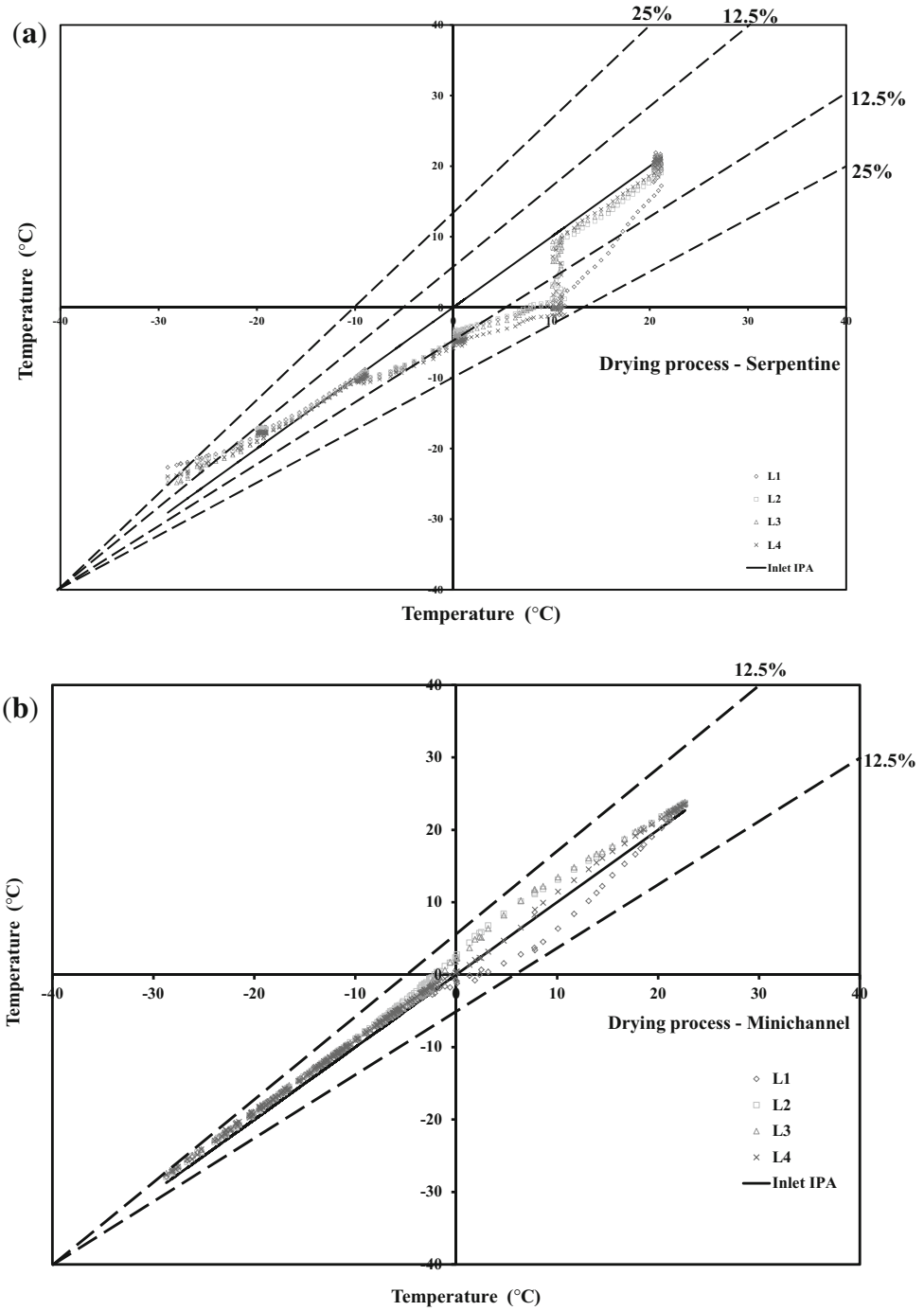

Figure 5. (**a**) Product temperature variation in drying process—serpentine channel. (**b**) Product temperature variation in drying process—mini-channel.

closest point to the end of secondary drying as the vacuum pump has very little water vapour to be pumped out, which results in a steep decline in the slope of the chamber pressure. This indication of pressure values during the end stage of the drying process can be used to determine the endpoint of drying. It is needless to mention that both pressure and temperature differences are the driving factors for sublimation and desorption phenomena to occur. To dry a sample of 150 ml of skimmed milk, the total drying time (primary drying and secondary drying) is 20709 s.

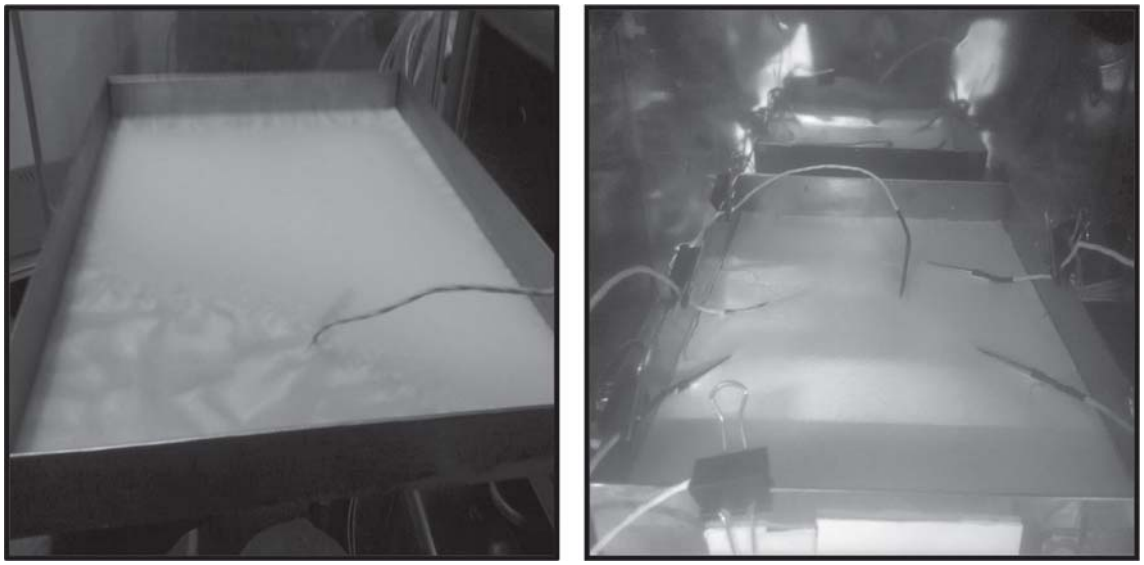

Figure 6. Ice layer uniformity in freezing stage—(**a**) serpentine, (**b**) mini channel.

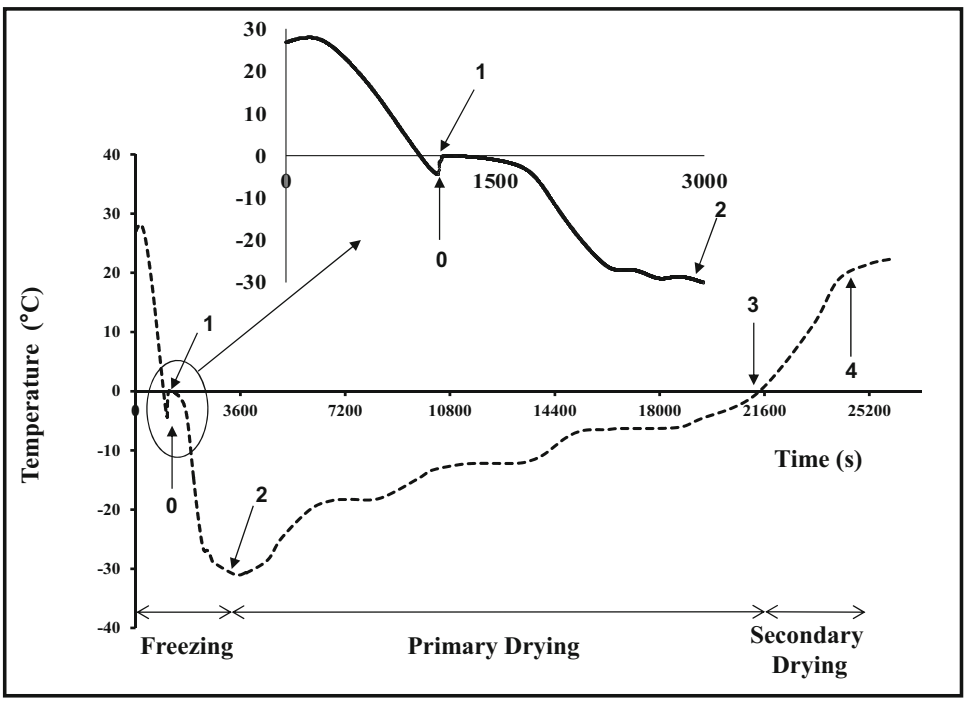

Figure 7. Cooling curve behavior in freezing process—mini channel.

3.4 *Determination of moisture content retention (X) and drying rate during the drying process*

The moisture ratio and drying rate achieved from mini channel configuration are shown in Figures 9 and 10. The individual runs are conducted for each hour, and the water content sublimated and desorbed is shown in table 2. The total drying time for complete sublimation and desorption of skimmed milk is 20710 s. The fraction of initial moisture content reduced to 50 % after 2 hours, as shown in figure 9. The drying rate is maximum at 0.032 kg h^{-1} after 1 hour at the initial stage of drying and reduces to 0.018 kg hr^{-1} at the end-stage, as shown in figure 10. Initially, the frozen layer is predominant during drying, and once the sublimation of water vapour starts, dry layer formation occurs. The dry layer begins to increase during the drying period

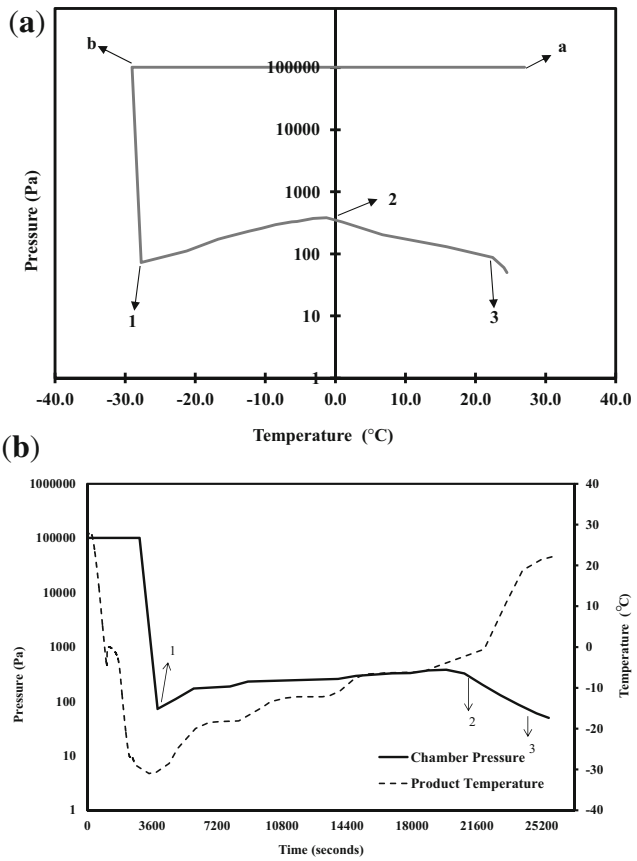

Figure 8. (**a**) Chamber Pressure agianst Product Temperature plot during drying process. (**b**) Chamber Pressure vs Product Temperature vs drying time.

gradually. The sublimated water content passes through the dry layer. The dried layer controls the product temperature and drying time. Hence drying rate reduces due to the presence of dry layer resistance, and similar observation is seen in the reduction of moisture content as 50 % of moisture content is sublimated in 2 hours, and the rest 50% takes nearly 4 hours to sublimate and desorb as shown in figure 9.

3.5 *Determination of heat load in the product during the drying process*

Based on the temperature difference between the heat exchanger fluid inlet and out (T_{FLO}-T_{FLI}) across the mini-channel shelf heat exchanger, the heat transferred is averaged between two-time intervals and is shown in Figure 11. There are three components, namely actual heat transferred, radiation heat transfer between the product and the surroundings and the net heat transferred which are determined using equations (1)-(3). Since drying takes the most time in the freeze-drying process, the heat transferred during primary and secondary drying alone is discussed.

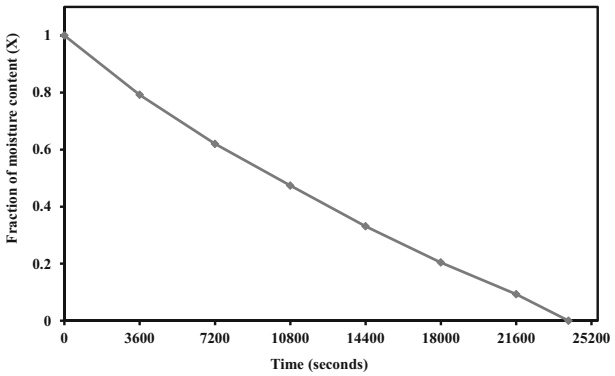

Figure 9. Variation of initial moisture content (X) during drying stage.

$$Q_{tot} = \dot{m} \times Cp \times (T_{FLo} - T_{FLi}) \quad (1)$$

$$Q_{rad} = \sigma \times A \times (T_{SU}^4 - T_{PRavg}^4) \quad (2)$$

$$Q_{act} = Q_{tot} - Q_{rad} \quad (3)$$

It can be observed from figure 11 that the magnitude of the total heat transferred is high during the earlier part of the drying process and subsequently decreases with time. Initially, the heat transferred reaches a peak value, which corresponds to the ramping of temperature in the shelf heat exchanger. For instance, for the tested condition, the total heat transferred reached a peak value of 97.06 W, which corresponds to rapid sublimation at the early stage of primary drying. Subsequently, from peak value, the heat transferred decreases to 42.48 W, which corresponds to the holding of temperature in the shelf heat exchanger. Upon ramping up the temperature again, the heat transfer reached the next peak value of 65.23 W. The decrease in heat transfer corresponds to the mass transfer resistance due to the dried layer, which is formed in the previous ramping and holding condition. As drying progresses, the thickness of the dried layer and mass transfer resistance also increases, which reflects in a low value of heat transfer. The highest value in the radiation component of heat transfer is 10 W, which is at the earlier stage of drying, where the temperature difference between the product temperature and the surrounding was around 40 °C. It reduces to 2 W at the end of the drying process, where the temperature difference also subsequently reduces to 7 °C. The influence of radiation effect in terms of the percentage of total heat load in the drying process increases gradually. During primary drying, heat load reaches an initial peak value of 97.06 W. The actual heat load contributes to 89.14 % (86.52 W), and radiation heat transfer adds 10.8% (10.91 W) to the total heat load at initial peak. At the end of primary drying, the actual heat load is at 75.55% (19.62 W), and radiation is at 24.4 % (6.3W). During the end of the secondary drying stage, the actual heat load is at 65.5 % (6.35W), and the radiation effect contributes to 34.4 % (3.34 W). The

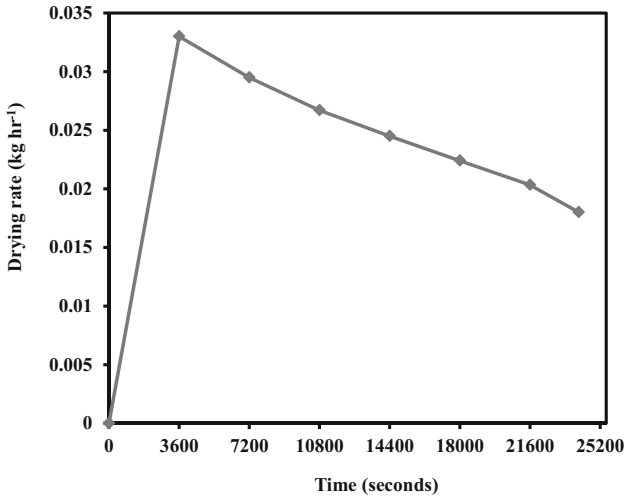

Figure 10. Variation in drying rate during drying process.

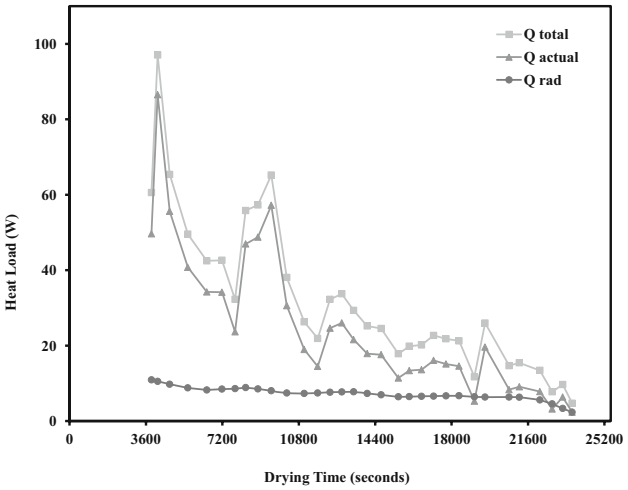

Figure 11. Determination of heat load in product during drying process.

decrease in the percentage of actual heat load contribution is attributed to the lower temperature difference between the inlet and outlet of isopropyl alcohol passing on the shelf. Hence a relative increase in the contribution of radiation heat transfer is reported at the end stage of primary drying and throughout the secondary drying process.

3.6 *Determination of overall heat transfer coefficient (K_v) and effectiveness of the mini-channel heat exchanger during the drying process*

The heat transfer coefficient and the effectiveness of the heat exchanger are determined using equations (4) and (5), are shown in Figure 12. The drying process is stopped during different time intervals, and the mass of the product present in the tray is measured along with water vapour condensed in the condenser chamber using a digital weighing scale. This assists in calculating the drying rate, moisture content retention, and overall heat transfer coefficient (K_v).

$$K_v = \frac{Q_{tot} \times Area}{T_{PRavg} - T_{FLavg}} \tag{4}$$

$$Effectivness = \frac{T_{FLi} - T_{FLo}}{T_{PRavg} - T_{FLi}} \tag{5}$$

The overall heat transfer coefficient (K_v) between two intervals is calculated as using above equation, where T_{FLavg} is the average fluid temperature in the heat exchanger, T_{PRavg} is the average temperature of the product, Q is total heat load, and A is an area of the shelf heat exchanger. It is seen that the maximum heat transfer coefficient lies at the initial stage of drying at 267 W m^{-2} k^{-1}. The heat transfer reduces during the holding part and increases during the next ramp. It lies in the range of 140–267 W m^{-2} k^{-1}. The effectiveness of the heat exchanger is calculated as $(T_{IN} - T_{OUT})/(T_{PR} - T_{IN})$, and the value varies between 0.7 to 0.05. During primary drying, the value is in the range between 0.5 and 0.7. The maximum effectiveness is at the beginning of the primary drying and decreases as the drying progresses. Further, the overall heat transfer coefficient and effectiveness values are higher during ramping and fall during the holding time, as shown in figure 12.

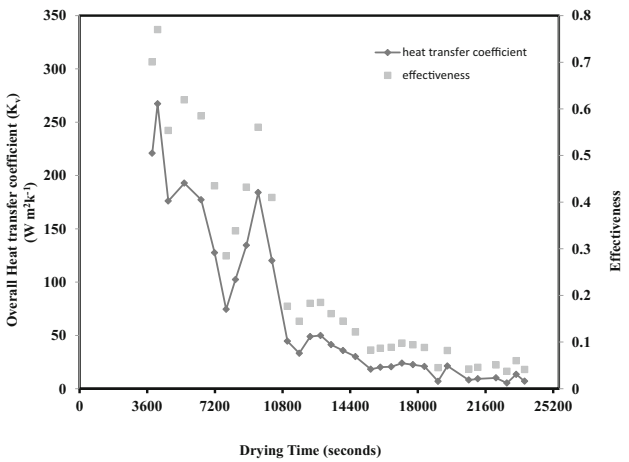

Figure 12. Determination of overall heat transfer coefficient (K_v) and effectiveness in drying process—mini channel.

4. Conclusions

An experimental study on a mini-channel heat exchanger as an alternative for the serpentine heat exchanger is studied for freeze dryer application.

- A comparison of the temperature plot of the product at various positions on both shelves is reported. During the freezing and drying stage serpentine channel showed higher temperature variation in a product higher than 75% and 25% when compared to mini-channel flow with 25% and less than 12.5%, respectively. Mini-channel reported minimal variation in product temperature and uniform ice layer throughout the shelf.
- The influence of chamber pressure and product temperature is analyzed to find the endpoint of drying, and it is found that both parameters are the driving forces for sublimation and desorption phenomena to occur. The drying rate is higher at the initial drying stage at 0.032 kg hr^{-1} after 1 hour and reduces as the dry layer formation starts. The fraction of moisture content decreases to 50% in 2 hours.
- In the case of heat load, the peak value is achieved at an early stage of drying due to the ramping effect and reduces during holding. The effect of radiation is relatively higher as it contributes to 31.51 % and 34 % of the total heat load during the end of primary drying and throughout the secondary drying process, respectively. The overall heat transfer coefficient lies in the range of 140–267 $Wm^{-2}k^{-1,}$ and effectiveness lie in the range of 0.7 to 0.5 in the primary drying phase.
- The ice layer obtained from the proposed mini channel shelf heat exchanger is uniform and thus assists in uniform drying of the product. The quality of the freeze dried product depends on the ice structure formed during freezing stage. The uniform ice structure obtained in mini channel shelf heat exchanger assists in proper drying, whereas serpentine forms wavy ice structure at corners. It is observed that the uniformity in temperature distribution in the product is achieved in both the freezing and drying stage using the proposed mini channel shelf heat exchanger. Thus mini-channel shelf is a suitable alternative for the serpentine shelf heat exchanger for the freeze-drying application.
- A general design procedure for the shelf heat exchangers used in the freeze-drying application is not available. It is important to mention that available literature on freeze drying either focuses on the process or on the product. In future work, the development and generalization of mini channel heat exchanger for the application in the freeze-drying process will be extensively analysed.

Acknowledgement

This work was supported by the Department of Science and Technology (DST-SERB), India (Ref no: SR/S3/MMER/0005/2014).

Nomenclature

D	diameter (mm)
Tg'	glass transition temperature (°C)
Δm	weight loss in product (kg)
T_{FLi}	isopropyl intlet temperature in the heat exchanger (°C)
T_{FLi}	isopropyl outlet temperature in the heat exchanger (°C)
T_{PRavg}	average temperature of the product at four locations (°C)
Q_{tot}	total heat load (W)
Qact	actual heat load (W)
Qrad	radiative heat load (W)
A	area of the shelf heat exchanger. (m^2)
K_v	overall heat transfer coefficient between heating liquid and product (W $m^{-2}K^{-1}$)
M	mass of sublimated water vapour (grams)
Cp	specific heat (J $kg^{-1}K^{-1)}$
σ	Stefan Boltzman constant
$\dot{m}$	mass flow rate Kg/s

Abbreviations

PT	pressure temperature
SM	skimmed milk
IPA	isopropyl alcohol
X	fraction of moisture Content
QBD	quality based design
SU	surroundings

References

[1] Ciurzynska A and Lenart A 2011 Freeze-drying-application in food processing and biotechnology—a review. *Pol. J. Food Nutr. Sci*. 61(3): 165–171

[2] Ratti C 2001 Hot air and freeze-drying of high-value foods: a review. *J. Food Eng*. 49(4): 311–319

[3] Panda H 2015 *Complete Hand Book on Frozen Food Processing and Freeze Drying Technology*.11th edition. Engineers India Research Institute

[4] Oetjen G W and Haseley P 2004 *Freeze Drying*. 2nd edition. Wiley, New York

[5] Hua T C, Liu B L and Zhang H 2010 *Freeze-Drying of Pharmaceutical and Food Products,* 1st edition. Elsevier, Amsterdam

[6] King C J 1970 *Freeze-drying of foodstuffs Critical Reviews in Food Technology*, 1st edition, CRC Press, Boca Raton

[7] Pham Q T 2014 *Food freezing and thawing calculations*. 1st edition. Springer, Berlin

[8] Rahman M S, Guizani N, Al-Khaseibi Md, Hinai S A A, Maskri S A A and Hamhami K A 2002 Analysis of cooling curve to determine the end point of freezing. *Food Hydrocoll*. 16(6): 653–659

[9] Rambhatla S, Ramot R, Bhugra C and Pikal M J 2004 Heat and mass transfer scale-up issues during freeze-drying: II. Control and characterization of the degree of super-cooling. *AAPS Pharm. Sci.Tech.* 5: 54–62.

[10] Rahman M S, Kasapis S, Guizani N and Al-Amri O S 2003 State diagram of tuna meat: freezing curve and glass transition. *J. Food Eng.* 57: 321–326

[11] Quast D G and Karel M 1968 Dry layer permeability and freeze-drying rates in concentrated fluid systems. *J. Food Sci*. 33: 170–175

[12] Hottot A, Vessot S and Andrieu J 2007 Freeze drying of pharmaceuticals in vials: Influence of freezing protocol and sample configuration on ice morphology and freeze-dried cake texture. *Chem. Eng. Process*. 46(7): 666–674

[13] Pikal M J, Roy M L and Shah S 1984 Mass and heat transfer in vial freeze-drying of pharmaceuticals: role of the vial. *J. Pharm. Sci.* 73(9): 1224–1237

[14] Bruttini R, Rovero G and Baldi G 1991 Experimentation and modelling of pharmaceutical lyophilization using a pilot plant, *Chem. Eng. J.* 45: 67–77

[15] Hottot A, Vessot S and Andrieu J 2005 Determination of mass and heat transfer parameters during freeze-drying cycles of pharmaceutical products. *PDA J. Pharm. Sci. Technol.* 59(2): 138–153

[16] Schneid S and Gieseler H 2008 Effect of Concentration, Vial Size and Fill Depth on Product Resistance of Sucrose Solutions During Freeze Drying. In: *Proc. 6th World Meeting on Pharmaceutics, Biopharmaceutics and Pharmaceutical Technology*, Barcelona, Spain

[17] Adhami S, Rahimi A and Hatamipour M S 2014 Comparison of quasi-steady-state and unsteady-state formulations in a freeze dryer modeling. *Heat Mass Transf.* 50(9): 1291–1300

[18] Pikal M J, Roy M L and Shah S 1998 Mass and heat transfer in vial freeze-drying of pharmaceuticals: Role of the vial. *J. Pharm. Sci*. 73(9): 1224–1237

[19] Sheehan P and Liapis AI 1998 Modelling of the primary and secondary drying stages of the freeze drying of pharmaceutical products in vials: Numerical results obtained from the solution of a dynamic and spatially multi-dimensional lyophilization model for different operational policies, *Biotechnol. Bioeng.* 60(6): 712–728

[20] Kobayashi M, Harashima K, Sunama R and Yao A R 1991 Inter-vial variance of the sublimation rate in shelf freeze-dryer. In: *Proceeding of 18th International Refrigeration Congress*, Saint Hyacinthe, Quebec, Canada, August 10–17: 1711–1715

[21] Sadikoglu H, Ozdemir M and Seker M 2003 Optimal control of the primary drying stage of freeze drying of solutions in vials using variational calculus. *Dry Technol.* 21(7): 1307–1331

[22] McWaid T and Marschall E 1992 Thermal contact resistance across pressed metal contacts in a vacuum environment; *Int. J. Heat Mass Transf.* 35(2): 2911–2920

[23] Gilmore D G 2002 *Spacecraft Thermal Control Handbook: Fundamental technologies*- (Chapter 16—M. B. H. Mantelli and M. M. Yovanovicht, Thermal Contact Resistance), 2nd edition, Aerospace Corp.

[24] Kandlikar S G, Garimella S, Li D, Colin S and King M 2006 *Heat Transfer and Fluid Flow in Minichannels and Microchannels* 1st edition. Elsevier, Amsterdam

[25] Kandlikar S G and Upadhye H R 2014 Extending the Heat Flux Limit with Enhanced Microchannels in Direct Single Phase Cooling of Computer Chips, In: *21st IEEE Sem-therm Symposium,* March 20–22, San Jose